

Features of dilute methane–oxygen flame front propagation towards combustible gas flow created by the fan

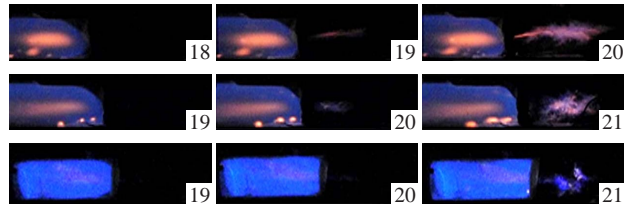
Nikolai M. Rubtsov,^{*a} Victor I. Chernysh,^a Georgii I. Tsvetkov^a and Kirill Ya. Troshin^b

^a A. G. Merzhanov Institute of Structural Macrokinetics and Materials Science, Russian Academy of Sciences, 142432 Chernogolovka, Moscow Region, Russian Federation. Fax: +7 496 524 6255; e-mail: nmrubtss@mail.ru

^b N. N. Semenov Federal Research Center for Chemical Physics, Russian Academy of Sciences, 119991 Moscow, Russian Federation. Fax: +7 499 137 2951; e-mail: troshin@center.chph.ras.ru

DOI: 10.1016/j.mencom.2024.06.035

Experiments with dilute methane–oxygen mixtures at pressures of 100–200 Torr on the flame front propagation towards the flow of combustible gas created by a fan showed that both the mean flame velocity and the length of the ‘flame jump’ through a hole in a flat obstacle increase with increasing counter flow velocity; *i.e.*, the flame accelerates towards the counter flow of combustible gas from the fan.



Keywords: methane, oxygen, flame jump, counter flow, acceleration, high-speed color filming.

The influence of different obstacles located in volumes filled with a combustible mixture on the propagation of the flame front (FF) has been studied for a long time.^{1,2} As is known, if the composition of the gas mixture is far from the ignition limits, then the velocity of the FF in the presence of obstacles can increase to supersonic values.^{3,4} The most prominent aspect in the investigation of these accelerated flames relates to explosion safety issues.⁵ If fire safety is violated, a certain amount of flammable gas may enter the surrounding air. The resulting explosive mixture can endanger the integrity of the vessel, reactor, mine, *etc.* The power of the explosion depends on the shape of the confinement and the number of openings in it, namely doors, windows and air vents.

The latter factor was taken into account,⁵ when the velocity distribution and motion of a whirling flame in a room with a vent were studied. The whirling flame model and crosswind velocity boundary conditions were used to study the velocity distribution of the rotating flame under the action of crosswind. The interaction of a single toroidal laminar vortex with a laminar premixed flame was investigated to determine the minimum size of the vortex that wrinkles the flame.⁴ Although the global characteristics of flame acceleration have been investigated by various authors,^{1,3–6} the database obtained by locally high-resolution measurements of process variables such as density, temperature, velocity and species concentration is still quite scarce. However, such data are very important for solving explosion safety problems, as well as for checking computer codes that simulate these accidents.

In accordance with the concept of the dependence of the flame penetration limit on the diameter of a single opening in the obstacle, there is a critical value of the opening diameter, below which the flame does not penetrate through the opening. However, we have previously shown that a diluted methane–oxygen flame penetrates through a close meshed grid, *i.e.*, through an obstacle consisting of a large number of openings of very small diameter.⁷ This means that the number of openings in the obstacle affects the limit of flame penetration through the obstacle. This matter, which is directly

related to explosion safety, is essentially not considered in the literature. We have experimentally demonstrated that when the FF penetrates through obstacles, gas-dynamic factors, such as flame turbulization, exhibit a noticeable feedback with the combustion kinetics.^{7,8} It has been established⁷ that after a single obstacle, FF does not occur in the immediate vicinity of the obstacle, and the primary center of ignition is observed far from the surface of the obstacle (‘flame jump’). It has been experimentally shown that when a flame penetrates through obstacles, gas-dynamic factors can determine the kinetic features of combustion, for example, the transition of low-temperature combustion of hydrocarbons to a high-temperature mode.⁷ Due to the complexity of branched chain combustion processes and the geometry of the confinement, flame propagation and the resulting warming-up cannot be simulated with suitable reliability. However, for this purpose, the compressible reactive Navier–Stokes equations can be simplified and used to model non-isothermal flow only if low Mach number flow is assumed.^{1,9,10} In low-velocity turbulent combustion applications, a variable density, low Mach number approximation of the Navier–Stokes equations is an adequate basis for modeling. Nevertheless, any comparison of the experimentally detected FF propagation with the result of numerical modeling is credible only in a qualitative aspect, *e.g.*, in terms of the velocity of propagation of the boundary between the initial and reacting gas, as well as in the shape of this boundary. As follows from the above, the effects of interaction between a premixed flame and a counter flow of combustible gas have not yet been thoroughly studied and understood. In addition, it is of interest to consider the possibility of interpreting the laws of interaction within the framework of a simplified two-dimensional problem.

This work is devoted to establishing the features of flame propagation in a dilute methane–oxygen mixture towards the flow of unreacted combustible gas created by a fan. It was also aimed at identifying the patterns and parameters that control flame penetration through flat obstacles, both with a central circular

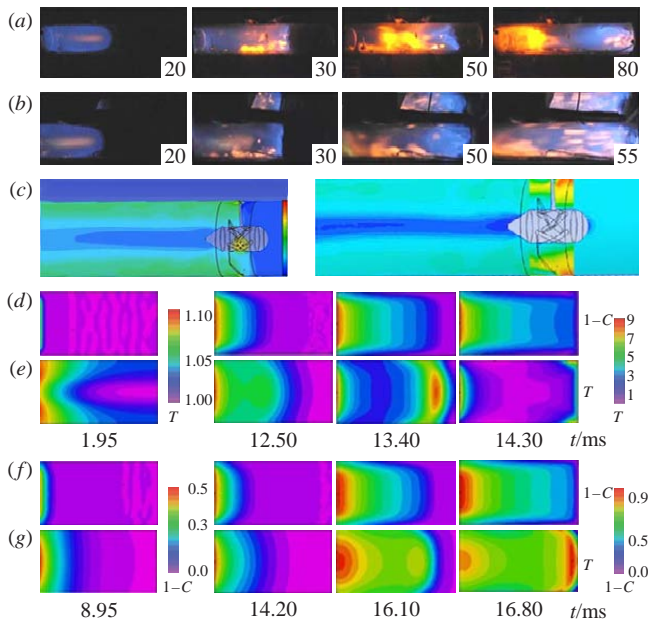


Figure 1 (a),(b) High-speed filming ($600 \text{ frames s}^{-1}$) of FF propagation in a cylindrical reactor at an initial pressure of 180 Torr with the fan turned (a) off and (b) on. The numbers on the frames are the frame numbers after ignition. (c) Distributions of gas pressure (left) and gas velocity (right) in the fan flow, calculated using ANSYS.¹¹ (d)–(g) Calculation of (d),(f) changes in the dimensionless degree of transformation ($1 - C$) of the initial substance \mathbf{C} with dimensionless concentration C and (e),(g) changes in the dimensionless temperature T during flame propagation with the fan turned (d),(e) on (2500 rpm) and (f),(g) off.

opening and with openings located asymmetrically relative to the reactor axis. This situation may arise when the combustion front propagates in residential and industrial premises. Thus, the features of the impact of the counter flow of combustible gas on the propagation of FF are relevant when solving fire safety issues.

Typical results of high-speed filming of FF propagation in a cylindrical reactor (Figure S1, see Online Supplementary Materials) are shown in Figure 1(a) with the fan turned off and in Figure 1(b) with the fan turned on. Thus, as one can see, the flame reaches the end of the reactor much earlier (in 55 frames) with the fan turned on than with the fan turned off (in 80 frames), that is, the counter flow of combustible gas provides a higher average flame velocity. In other words, the flame accelerates towards the flow of unreacted gas.

Figure 2 shows typical high-speed frame sequences of FF penetration through a flat obstacle 14 cm in diameter with one opening in the center 22 mm in diameter. The frames in Figure 2(a) were taken at a fan rotation speed of 2500 rpm, the frames in Figure 2(b) correspond to half the rotation speed, and Figure 2(c) reflects the processes occurring when the fan is turned off. When comparing Figures 2(a) and 2(b), it can be seen that the higher the fan speed, the longer the ‘flame jump’.

Figure 3 displays a typical frame sequence of high-speed filming of FF penetration through a flat obstacle 14 cm in diameter with two asymmetrically arranged circular openings 20 mm in diameter (the first opening is located in the center of the obstacle, and the second is at a distance of 40 mm from the center). As can be seen in the Figure, flames after an obstacle propagate along curved trajectories, whereas in the absence of a current gas flow, these flames propagate almost rectilinearly (see Figure 1(a),(b), frame 20 elsewhere⁸).

Given the available fan speeds and power, it was not possible to experimentally determine the possibility of flame blow-off under the conditions of our experiment.

Note that the problem of the impact of a counter flow of combustible gas on a propagating flame is multifactorial: the counter

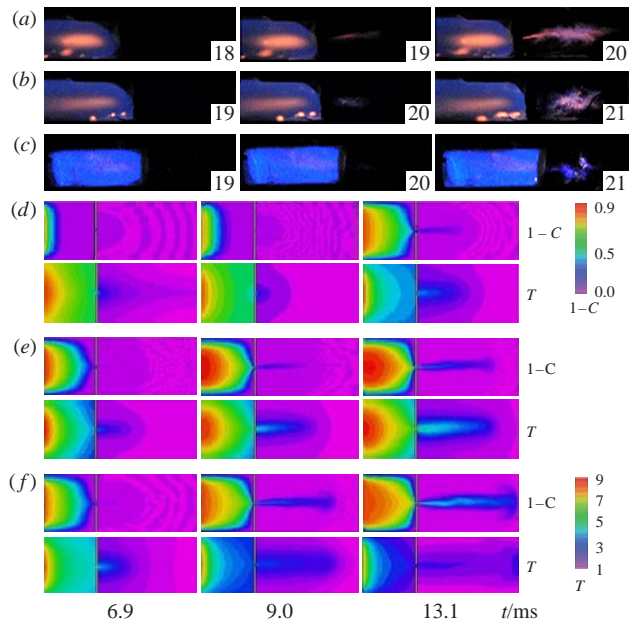


Figure 2 (a)–(b) High-speed filming of FF penetration through a flat obstacle 14 cm in diameter with one central opening 22 mm in diameter with the fan turned on at a speed of (a) 2500 or (b) 1250 rpm and (c) turned off. (d)–(f) Results of calculating the dimensionless degree of transformation ($1 - C$) of the initial substance \mathbf{C} and the dimensionless temperature T during flame penetration through an opening with a diameter of 0.02 of the channel diameter. The boundary conditions on the right boundary of the channel, simulating the flow from the fan, are as follows: $u = A[1.1 - \cos(y - 0.5)]$, $v = 0$ and $\rho = A[1.1 - \cos(y - 0.5)]$, where u and v are the velocity components in the x and y directions, respectively, with (d) $A = 0$, (e) $A = 5 \times 10^{-4}$ or (f) $A = 1 \times 10^{-3}$.

flow of gas introduces additional fuel and oxidizer, and also perturbs and increases the flame surface. These factors should lead to an increase in the flame propagation velocity. However, this is not the case, since, as can be seen from Figure 1, there is no noticeable disturbance on the surface of the flame propagating towards the fan [Figure 1(a), frame 30] compared to a freely propagating flame [Figure 1(b), frame 30]. Further, the surfaces of both flames are disturbed due to interaction with the end wall.¹² Therefore, it is necessary to take into account the parameters of the counter flow of gas from the fan, which has a characteristic distribution along the diameter of the channel. Below, to describe the qualitative regularities of the process, we took into account the distribution of velocity and temperature created by the fan along the diameter of the reactor.

Thus, above we illustrated some features of flame penetration through the obstacles under study by numerical modeling using compressible dimensionless reactive Navier–Stokes equations in the low Mach number approximation,^{13,14} which describe flame propagation in a two-dimensional channel. The obtained results showed qualitative agreement with the experiments.^{7,8} The problem was solved by the finite element analysis using the FlexPDE 6.08 software package (PDE Solutions Inc., 1996–2008).¹⁵ A simple chain mechanism^{7,8} was used. The initiation condition was taken to be $T = 10$ on the left boundary of the channel, as well as $\rho = A[1.1 - \cos(y - 0.5)]$ and $u = A[1.1 - \cos(y - 0.5)]$ on the right boundary of the channel, while the restriction $1 \times 10^{-4} < A < 1 \times 10^{-3}$ was imposed on the coefficient A , and there was an obstacle in the channel. The boundary conditions (including the orifice) were $C_\xi = 0$, $u = 0$, $v = 0$, $\rho_\xi = 0$ and $n = 0$ (type I boundary conditions) only on the obstacle surface, and also allowed convective heat exchange $T_t = T - T_0$, where ξ is the dimensionless coordinate.

An approximate description of the gas flow created by the fan was obtained as a result of a numerical solution of this problem

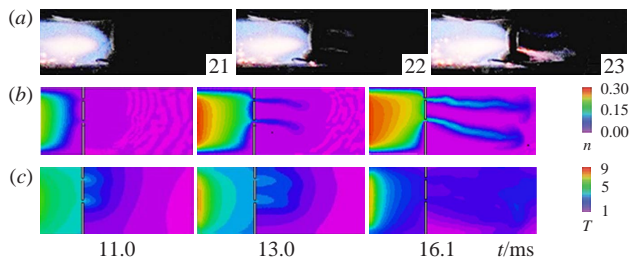


Figure 3 (a) High-speed filming of FF penetration through a flat obstacle 14 cm in diameter with two asymmetrically arranged circular openings 20 mm in diameter, located in the center and at a distance of 40 mm from it, with the fan turned on at a speed of 2500 rpm. (b),(c) Modeling the process of flame propagation with the fan turned on in terms of (b) changes in the dimensionless concentration n of the active intermediate and (c) changes in the dimensionless temperature T .

using the ANSYS Fluent software package.¹¹ The fact that under the experimental conditions there is a stationary steady-state flow from the fan allows us to qualitatively consider this flow in two-dimensional form. Figure 1(c) shows two-dimensional profiles of temperature and fan speed (780 rpm, $15.6 \text{ m}^3 \text{ s}^{-1}$, 724 mm H₂O) as calculated in the ANSYS Fluent software environment.¹¹ A similar profile occurs for gas density.¹¹ These profiles were considered in the initial and boundary conditions for gas density and velocity v_x . It was found that the calculated dependences presented in Figure 1(c) can be satisfactorily approximated by simple harmonic functions for a low-power fan. It was shown that it is enough to take into account the initial and boundary conditions with the fan turned on as $par = A[1.1 - \cos(y - 0.5)]$, where par is ρ or u and A is a dimensionless coefficient.

The results of qualitative calculations of flame propagation towards the fan are presented in Figures 1(d)–(g), 2(d)–(f) and 3(b), (c). As can be seen, the results of the analysis are in qualitative agreement with the experiment presented in the Figures. Indeed, the results of calculating the dimensionless degree of transformation $(1 - C)$ of the initial substance C and the dimensionless temperature T show that both the mean flame velocity [Figure 1(a), (b)] and the length of the ‘flame jump’ increase if the fan is turned on, and the higher the fan speed, the longer the ‘flame jump’ (Figure 2).

The results of qualitative modeling of flame penetration through two asymmetrically openings show that the flame trajectories are consistent with the experimental ones, and at the same time, these trajectories are qualitatively different from the trajectories of FF penetration through symmetrical openings.^{8,13}

In summary, the experiments on the propagation of a flame front in a dilute methane–oxygen mixture at 100–200 Torr towards the flow of combustible gas generated by a fan have shown that both the average flame velocity and the length of the ‘flame jump’

through an opening in a flat obstacle increase with increasing the speed of the counter flow of unreacted combustible gas, *i.e.*, the counter flow of combustible gas from the fan accelerates the flame. Qualitatively, this result can be described by taking into account the distribution of temperature and velocity caused by the fan along the diameter of the reactor. The obtained result is important for solving explosion safety problems in complex volumes.

Online Supplementary Materials

Supplementary data associated with this article can be found in the online version at doi: 10.1016/j.mencom.2024.06.035.

References

1. C. Gerlach, A. Eder, M. Jordan, N. Ardey and F. Mayinger, in *Heat Transfer Enhancement of Heat Exchangers*, eds. S. Kakaç, A. E. Bergles, F. Mayinger and H. Yüncü, Springer, Dordrecht, 1999, pp. 395–406.
2. N. M. Rubtsov, V. I. Chernysh, G. I. Tsvetkov and K. Ya. Troshin, *Mendeleev Commun.*, 2017, **27**, 101.
3. Q. Duan, H. Xiao, W. Gao, L. Gong and J. Sun, *J. Hazard. Mater.*, 2016, **320**, 18.
4. W. L. Roberts and J. F. Driscoll, *Combust. Flame*, 1991, **87**, 245.
5. Z. Gao, S. S. Li, Y. Gao, H. Y. Hung and W. Chow, *Building Simulation*, 2021, **14**, 1499.
6. Ya. B. Zeldovich, G. I. Barenblatt, V. B. Librovich and G. M. Makhviladze, *Matematicheskaya teoriya goreniya i vzryva (Mathematical Theory of Combustion and Explosion)*, Nauka, Moscow, 1980 (in Russian).
7. N. M. Rubtsov, V. I. Chernysh, G. I. Tsvetkov and K. Ya. Troshin, *Mendeleev Commun.*, 2023, **33**, 279.
8. N. M. Rubtsov, V. I. Chernysh, G. I. Tsvetkov and K. Ya. Troshin, *Mendeleev Commun.*, 2018, **28**, 99.
9. S. Chakraborty, A. Mukhopadhyay and S. Sen, *Int. J. Therm. Sci.*, 2008, **47**, 84.
10. V. Polezhaev and S. Nikitin, in *Proceedings of 16th International Congress on Sound and Vibration, ICSV 2009*, International Institute of Acoustics and Vibrations, Auburn, AL, 2009, vol. 3, pp. 1592–1598.
11. [dataset] A. Abdulin, *Modelirovaniye techeniya vozdukh v osevom ventilyatore v ANSYS CFX (Simulation of Air Flow in an Axial Fan in ANSYS CFX)*, Videourok ANSYS CFX, 2020, <https://www.youtube.com/watch?v=FeNbbIvQB7Y> (in Russian).
12. V. Akkerman, V. Bychkov, A. Petchenko and L.-E. Eriksson, *Combust. Flame*, 2006, **145**, 675.
13. N. M. Rubtsov, V. I. Chernysh, G. I. Tsvetkov and K. Ya. Troshin, *Mendeleev Commun.*, 2023, **33**, 433.
14. A. Majda, *Compressible Fluid Flow and Systems of Conservation Laws in Several Space Variables*, Springer Science+Business Media, New York, 1984.
15. G. Backstrom, *Simple Fields of Physics by Finite Element Analysis*, GB Publishing, Malmö, Sweden, 2005.

Received: 5th February 2024; Com. 24/7383